Russian Geology and Geophysics © 2020, V.S. Sobolev IGM, Siberian Branch of the RAS
Vol. 61, No. 7, pp. 700–714, 2020 *DOI:10.15372/RGG2019158* *Geologiya i Geofizika*

Stages of Volcanic Activity on the Southeastern Flank of the Sredinny Range (Kamchatka): Age, Geochemistry, and Isotopic Characteristics of Volcanic Rocks of the Akhtang and Kostina Mountain Massifs

A.O. Volynets[a, ✉], M.M. Pevzner[b], V.A. Lebedev[c], Yu.V. Kuscheva[b], Yu.V. Gol'tsman[c], Yu.A. Kostitsin[d], M.L. Tolstykh[d], A.D. Babansky[c]

[a] *Institute of Volcanology and Seismology, Far Eastern Branch of the Russian Academy of Sciences, bul'v. Piipa 9, Petropavlovsk-Kamchatsky, 683006, Russia,*

[b] *Geological Institute, Russian Academy of Sciences, Pyzhevskii per. 7, Moscow, 119017, Russia*

[c] *Institute of Geology of Ore Deposits, Petrography, Mineralogy and Geochemistry, Russian Academy of Sciences, Staromonetnyi per. 35, Moscow, 119017, Russia*

[d] *Vernadsky Institute of Geochemistry and Analytical Chemistry, Russian Academy of Sciences, ul. Kosygina 19, Moscow, 119091, Russia*

Received 19 February 2019; received in revised form 8 August 2019; accepted 10 October 2019

Abstract—We report the chemical and isotopic compositions of volcanic rocks of the Akhtang and Kostina mountain massifs in the Sredinny Range, Kamchatka. The analyzed rocks are similar in composition to the earlier studied volcanics of the eastern flank of the southern part of the Sredinny Range. Results of K–Ar isotope dating reveal three stages of volcanic activity in the two massifs. These stages are divided by long (1.4 and 2.4 Ma) periods of quiescence. In the Akhtang massif, the eruptive activity was at 4.9–4.0, 1.9–1.7, and 0.3–0.2 Ma, and in the Mt. Kostina massif, at ~8.0, 5.6–4.9, and ~3.5 Ma. Two early stages of both massifs are characterized by the eruption of island arc type rocks, and the late stage, by the eruption of rocks of hybrid geochemical type. The Mio-Pliocene (N_1–N_2^1) rocks of the Mt. Kostina massif are similar in geochemical features to the early Pliocene (N_2^1) rocks of the Akhtang massif, and the late Pliocene (N_2^2) lavas of the former massif are similar to the middle Quaternary (Q_2) rocks of the superimposed monogenetic volcanism zone of the latter massif. For the Akhtang massif it has been first discovered that the volcanic reactivation after the long quiescence periods was accompanied by a change in the composition of rocks and in the type of eruptive activity (from the eruption of plateau-effusives rocks to the formation of stratovolcanoes and monogenetic volcanism zones). The obtained data on the age and composition of rocks as well as some morphological features of the studied massifs suggest that the plateau-effusive rocks of the Sredinny Range might be related to central-type eruptions.

Keywords: island arc and hybrid volcanism, subduction, Sr and Nd isotopes, K–Ar dating, geochemistry, Sredinny Range, Kamchatka, Akhtang and Kostina volcanic massifs

INTRODUCTION

The Sredinny Range (SR) is one of the least studied volcanic regions of Kamchatka. Most researchers agree that during the pre-late Miocene time volcanism in the SR was caused by the subduction of the Pacific plate with the trench located 200 km to the west from its contemporary position (Legler, 1977; Konstantinovskaya, 1999; Shapiro and Lander, 2003; Avdeiko et al., 2006). During the late Miocene–Pliocene the subduction under the SR was blocked due to the accretion of the Kronotsk arc (Legler, 1977; Shapiro and Lander, 2003). A new zone of the Pacific plate subduction was formed near the eastern shore of Kamchatka, and it causes the contemporary volcanic activity in the Eastern volcanic belt and in the Central Kamchatka Depression. The reasons of the Pliocene–Quaternary activity in the SR are still under discussion (Volynets, 1993, 1994; Tatsumi et al., 1995; Churikova et al., 2001; Avdeiko et al., 2002, 2006; Perepelov et al., 2006; Plechov, 2008; Avdeiko and Palueva, 2009; Volynets et al., 2010; Koloskov et al., 2013; Perepelov, 2014; Nekrylov et al., 2015; Nerkylov et al., 2018; Volynets et al., 2018).

From a geomorphological point of view, the SR may be divided into two parts according to its structure: northern and southern (Fig. 1). The northern part of the SR is a narrow range stretching to NE. The southern part has a more complicated structure. There are two or even three elements in it: (1) "eastern" flank stretching to NE (Kozyrevsky and Bystrinsky Ridges), which is a continuation of the northern part of the Range; and (2) "western" flank, which diverges

✉ Corresponding author.
E-mail address: a.volynets@gmail.com (A.O. Volynets)

like a fan from the Sredinny metamorphic massif to NNE and is marked by the large volcanic massifs[1] – Khangar, Ichinsky, Kekuknaysky, and Ketepana. The Anaunsky Dol, Uksichan and Bolshoy Chekchebonay volcanic massifs are located in between and probably mark the third, "central", flank of the southern part of the SR. This subdivision was confirmed by geochemical research (Volynets et al., 2018). In the northern part of the SR, typical island-arc rocks were erupted in the Mio-Pliocene; they have been changed by the hybrid type volcanic rocks with a high degree of enrichment in the Quaternary (Volynets et al., 2010) (we call rocks "hybrid" when they combine island arc and within-plate affinities (i.e. simultaneous increase of HFSE and LILE concentrations); the degree of enrichment relative to MORB is estimated by HFSE content (Churikova et al., 2001; Volynets et al., 2010)). In the "eastern" flank of the southern part of the SR, rare finds of rocks with confirmed Miocene age are also characterized by the island arc type of microelements distribution, while in the Pliocene–Quaternary there are eruptions close in space and time of both island arc and hybrid types with a low degree of enrichment (Volynets et al., 2018). In the "western" flank of the southern part of the SR, only hybrid type rocks are present since the late Miocene (Pevzner et al., 2017; Volynets et al., 2018). Pliocene–Quaternary volcanic rocks of the "central" flank (Anaunsky Dol, Uksichan and Bolshoy Chekchebonay) are close in geochemistry to the rocks of the "eastern" flank of the southern part of the SR (Volynets et al., 2018). According to (Gorbatov et al., 1997), the slab is located at a ~300 km depth under the volcanoes of the "eastern" flank of the southern part of the SR up to the latitude of the Bystraya River (Fig. 1); in the "western" flank, the Benioff zone is visualized under the Khangar volcano at 400 km depth and is not found further to the north.

Akhtang Mountain (N 55.426609º, E 158.653977º, 1954.6 m, Fig. 1) is the largest summit of the Kozyrevsky Ridge in the "eastern" flank of the southern part of the SR. This volcano is located at the watershed of the Sukhariki and Karakovaya rivers. The zone of monogenetic volcanism crosses its slopes and pedestal in the NE direction. Single geochemical analyses from this area were published in (Churikova et al., 2001) and in the explanatory note to the State geological map (Khasanov et al., 2008). No systematic research of the composition of volcanic rocks was done here. According to the data from the geological map, plateau-effusives of the massif pedestal were formed in early Quaternary, and the stratovolcano – in late Quaternary; superimposed zone of monogenetic volcanism is considered Holocene age

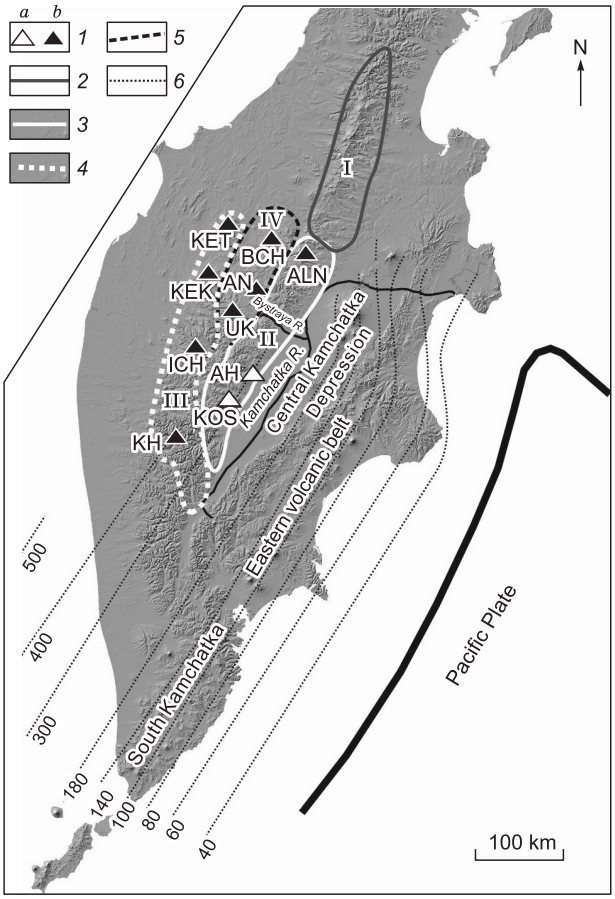

Fig. 1. Scheme of Sredinny Range and location of the objects of study. Legend: *1*, volcanic massifs (a, objects of this study, b, mentioned in text): KOS, Kostina Mt.; AH, Akhtang; ALN, Alney-Chashakondzha; KH, Khangar; ICH, Ichinsky; KEK, Kekuknaysky; KET, Bolshaya Ketepana; UK, Uksichan; AN, Anaunsky Dol; BCH, Bolshoy Chekchebonay; *2–5:* supposed division of the SR (Volynets et al., 2018): *2*, northern part (I); *3–5*, southern part: *3*, "eastern" flank (II); *4*, "western" flank (III); *5*, "central" flank (IV); *6*, depth (km) to the roof of the subducting Pacific plate after (Gorbatov et al., 1997). The northern part together with the "eastern" flank of the southern part (I and II) form the main watershed of the Sredinny Range. The thick black line shows the location of the deep-water trench of the Kuril-Kamchatka subduction zone.

(Khasanov et al., 2008). Similar estimates on the age are provided in (Ogorodov et al., 1972): the Akhtang Volcano is late Quaternary, the monogenetic zone – Holocene.

Kostina Mountain (N 55.153224º, E 158.110016º, 1752.5 m, Fig. 1) is located in the "eastern" flank of the southern part of the SR in 45 km to the SW from the summit of the Akhtang Volcano at the watershed of the Balkhach and the Lev. Kirganik rivers. It is a substantially destroyed volcanic edifice, composed mainly by lavas. Data on age (Pliocene) and composition of rocks are available only from the explanatory note to the State geological map (Khasanov et al., 2009). We include volcanic rocks of the nearby located Zagadka and Kubinskaya mountains in the Kostina Mt. massif.

[1] The term "volcanic massif" is referred to the group of closely spaced edifices built by volcanic rocks of different geochemical types, formed during different times. The individual massif may include several structural elements: plateau-effusives, stratovolcano, superimposed zone of monogenetic scoria cones, caldera, etc. A massif is named after the main summit of the complex of the volcanic edifices. Therefore a massif is a group of volcanoes of different age, which are compactly located within the same area.

Zagadka Mountain (N 55.158405º, E 158.276026º, 1583.1 m) is situated 11 km to the east from Kostina Mountain at the watershed of the Balkhach and the Mal. Kimitina rivers. It is a strongly eroded gently sloping plateau-like surface, composed by lavas. According to (Khasanov et al., 2009) these volcanic rocks were formed during the early Quaternary and are underlain by middle Miocene rocks with disconformity.

Kubinskaya Mountain (N 55.070823º, E 158.216478º, 1229.0 m) is located 11 km to the SE from Kostina Mt. in the upstream of the Mal. Kimitina river. This mountain is an elongated to the SE edifice with a plateau-like surface. The age of Kubinskaya Mt. is Eopleistocene according to (Khasanov et al., 2009).

The goal of this research was to study the evolution of magmatism and to determine the age of formation of various objects from two volcanic massifs – Akhtang and Kostina. To achieve this goal we accomplished geological-geomorphological mapping with interpretation of the large-scale aero-photo images, which allowed us to find several structural elements which were presumably formed at different times. During the field works we gathered a collection of volcanic rocks from which later we obtained a representative set of data on the geochemical composition and isotopic K-Ar age of rocks of two volcanic massifs of the southeastern wing of the Sredinny Range of Kamchatka.

ANALYTICAL METHODS

Concentrations of major, minor and select trace elements (V, Cr, Co, Ni, Cu, Zn, Rb, Sr, Y, Zr, Nb, Ba, Pb) were analyzed by X-ray fluorescence spectroscopy (XRF) using an Axios MAX vacuum sequential spectrometer (wavelength dispersive) made by PANalytical at the CKP "IGEM-Analytika" at the Institute of Geology of Ore Deposits, Petrography, Mineralogy, and Geochemistry, Russian Academy of Sciences (IGEM RAS), analyst A.I. Yakushev. For determination of the major elements, glass disks were prepared by the induction melting of the annealed sample powders mixed with lithium borates at 1200 °C. For the determination of the trace elements, samples were prepared by cold pressing the dry powders with plastic filler in a tablet 32 mm in diameter. Analytical errors were 1–5% for the elements with concentrations >0.5 wt.% and up to 12% for the elements with concentrations < 0.5 wt.%.

Additional trace elements were analyzed by inductively coupled plasma mass spectrometry (ICP-MS) at the Institute of Microelectronics, Technology, and High Purity Materials RAS (IMT RAS) using a mass spectrometer with inductively coupled plasma X-7 (Thermo Elemental, USA), analyst V.K. Karandashev. Powdered samples were digested in an acid mixture following standard procedures described by Karandashev et al. (2008). The accuracy of the measurements was monitored by analyzing USGS standards BHVO-2, BIR-1, AGV-2, GSP-2 and in-house reference materials (Jochum et al., 2016; Karandashev et al., 2016). The accuracy for most trace elements was ~ 7%.

Representative samples were analyzed for Sr and Nd isotopic composition. Measurements were done in the laboratories of isotopic geochemistry and geochronology of Vernadsky Institute of Geochemistry and Analytical Chemistry RAS (GEOHI RAS) and IGEM RAS. Extraction of Nd and Sr was made by standard method after the dissolution of samples in the $HF+HNO_3$ mixture using column chromatography. In GEOHI RAS, the isotopic analyses were done at mass-spectrometer Triton TI. Measured values of JNd1 and SRM-98 standards were 0.512108±16 and 0.710236±12. All errors discussed in this paper are within the 2σ range. In IGEM RAS, Sr and Nd isotopes were measured at multicollector thermoionization mass-spectrometer "Sector 54" (Micromass, UK). The correctness of measurements of isotopic ratios $^{87}Sr/^{86}Sr$ and $^{143}Nd/^{144}Nd$ was controlled by systematic analyses of the international standard of Sr (SRM-987) and in-house Nd isotopic standard "Nd-IGEM" which is calibrated to La Jolla international standard. The error of the measured $^{87}Sr/^{86}Sr$ and $^{143}Nd/^{144}Nd$ does not exceed 0.003%. For isotopic ratios $^{87}Rb/^{86}Sr$ and $^{147}Sm/^{144}Nd$ errors were 1% and 0.2%, respectively (2σ). This method is reported in (Chernyshov et al., 2012).

Radiogenic argon measurements in the samples from the Akhtang massif, Kostina and Kubinskaya mountains were conducted in the laboratory of isotopic geochemistry and geochronology of IGEM RAS on the mass-spectrometer complex MI-1201 IG using the method of isotopic dilution with ^{38}Ar as a tracer; potassium content was determined by flame spectrophotometry (Lebedev et al., 2010). The groundmass of rocks were used for analyses. Samples from Zagadka Mountain and Uglovoy stream were measured for radiogenic argon in the laboratory of isotopic geochemistry and geochronology in the Geological Institute RAS (GIN RAS) in whole-rock samples (160–190 mg) on the mass-spectrometer complex MI-1201 IG by isotopic dilution method. Samples were melted at 1600–1800 °C. Clearness of tracer – monoisotope ^{38}Ar – was 97.5%. The fraction of air argon was 60–90%. Potassium concentration was measured by atomic absorber AAS-3 in the chemical-analytical laboratory of GIN RAS by I.V. Kislova, the error is less than 1%. Both laboratories used the following constants to calculate the age: $\lambda e = 0.581 \times 10^{-10}$ year^{-1}; $\lambda\beta = 4.962\times10^{-10}$ year^{-1}; $^{40}K/K = 1.167\times10^{-4}$ (Steiger and Jager, 1977).

RESULTS

Concentrations of major and microelements in the studied rock and geographical locations of the sampling sites are presented in the Supplementary material (http://sibran.ru/journals/supp_mateirals.xlsx).

Age of volcanic rocks. *Akhtang massif.* During the interpretation of the large-scale aero-photo images we have found several groups of volcanic rocks, which substantially differ by their preservation. The strongest denudation (intensive breakdown, steep cliffs, absence of the primary volcanic relief) is typical for plateau-effusives, which are repre-

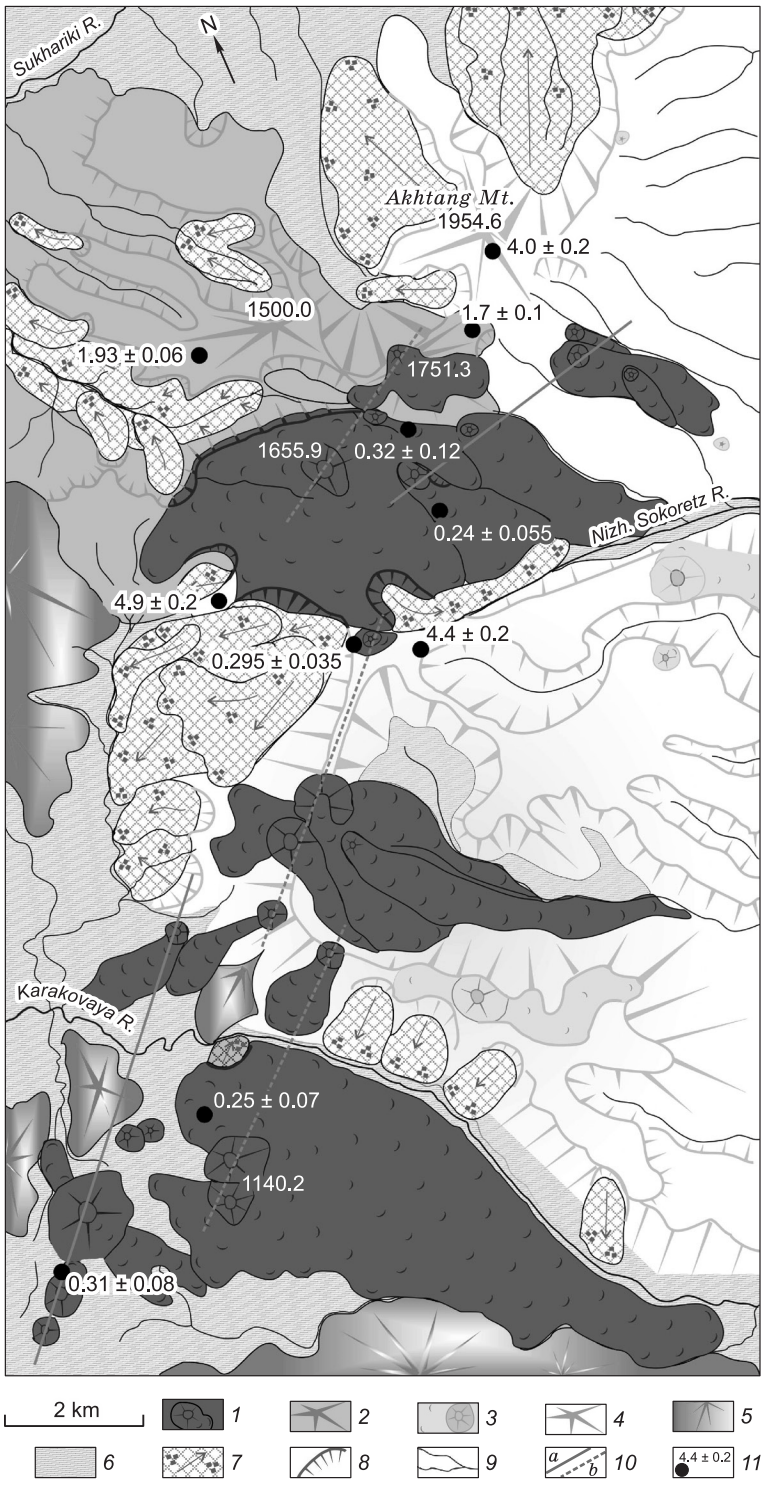

Fig. 2. Geological-geomorphological scheme of the Akhtang volcanic massif. 1, Middle Pleistocene volcanic rocks, including scoria and lava-scoria cones and their lava flows; 2, early Pleistocene volcanic rocks, star indicates the summit of the preserved edifice; 3, scoria cones and lava flows with unknown age on undivided Pliocene rocks; 4, Pliocene volcanic rocks, star indicates the summit of the preserved edifice; 5, rocks of Neogene age, undivided; 6, contemporary alluvial-peat bog and volcanogenic-proluvial deposits; 7, collapses and moraines of different age, arrow indicates the direction of collapse; 8, cliffs and slopes, colors refer to the volcanic complexes of different age; 9, contemporary rivers; 10, supposed position of the main linear stretching zones, which are connected to the chains of monogenetic centers, with rocks of: a, island arc type; b, hybrid type; 11, sampling sites and K-Ar age (Ma) according to Table 1.

sented by the gently sloped aligned surfaces. They compose the massif pedestal and are best preserved at its eastern foot (Fig. 2). There are several poorly preserved lava centers on the surface of the plateau, which we failed to sample. The Akhtang stratovolcano (1954.6 m) – the main summit of the massif – was formed at the surface of this plateau; there are reduced fragments of primary relief on its slopes. The northern sector of the volcano edifice is substantially destroyed. The NE part of the collapse circuses, opened to the north, is occupied by collapse and moraines deposits with typical hilly-sinkhole and hilly relief; in the NW part there is a large lava center with maximal height ~1500 m. This center is also substantially destroyed and complicated by numerous collapse circuses; valleys of the transversal streams are partly filled with collapse-loose deposits. The best morphological preservation is observed for numerous scoria (scoria-lava) cones and their lava flows. Many cones still have craters preserved, and fragments of longitudinal and transversal flow shafts are visible on the lava flows. Cones form a zone, which crosses the massif in the northeastern direction from the right bank of the Karakovaya River to the right bank of the Sukhariki River.

We have done K-Ar isotopic dating of volcanic objects, which differ by the type of eruptive activity, morphological shape and degree of denudation (Table 1). It is obvious from Table 1 that the results are divided into three rather compact age groups: early Pliocene (hereafter – Pliocene), early and middle Quaternary. The remaining (undated) volcanic rocks were referred to established age groups by their morphological characteristics, and by the results of comparison of the major and microelement composition of these rocks with the isotopically dated samples. Our research allowed us to distinguish three stages of volcanic activity with the dividing quiescence periods in the geological history of the Akhtang massif, which were documented for the first time.

The beginning of activity (stage I, N_2) is referred to the early Pliocene (4.9–4.0 Ma, Table 1). It is very likely that this stage consists from two successive phases. During the early phase (4.9–4.3 Ma) plateau-effusives were erupted (they are now widely represented at the eastern, and to the less extent, at the western sector of the massif). During the final phase (about 4.0 Ma) the Akhtang stratovolcano was formed (1954.6 m) (Fig. 2).

After the period of rest which lasted about 2 m.y. a second stage of activity started (stage II, Q_1) – early Pleistocene (1.9–1.7 Ma, Table 1). At the beginning, a lava volcano (~1500 m) was formed at the WNW sector of the massif in the large collapse circus of the Pliocene edifice; at the end –

Table 1. Results of K-Ar isotopic dating of the volcanic rocks of Akhtang and Kostina Mt. massifs

Samples		Coordinates (° N)	Coordinates (° E)	Height (m)	Potassium, % ± σ	$^{40}Ar_{rad}$ (ng/g) ± σ	$^{40}Ar_{air}$ (%) in sample	Age, Ma ± 2σ	Stage
№ lab.	№ field								
Akhtang massif									
16152	AX-1302	55.40142	158.61640	1545	0.845 ± 0.015	0.0139 ± 0.0017	97.9	0.24 ± 0.055	
16147	AX-1353	55.33468	158.50612	1069	1.35 ± 0.02	0.023 ± 0.003	98.2	0.25 ± 0.07	
16150	AX-1343	55.38068	158.57943	1501	1.17 ± 0.02	0.0238 ± 0.0013	88.9	0.295 ± 0.035	Q_2 (III)
16151	KAR-1301	55.33071	158.46967	1041	1.06 ± 0.02	0.023 ± 0.003	98.1	0.31 ± 0.08	
16149	AX-1337	55.40611	158.62728	1449	1.18 ± 0.02	0.026 ± 0.005	98.6	0.32 ± 0.12	
16203	AX-1326	55.41962	158.63843	1574	1.15 ± 0.02	0.133 ± 0.002	79.3	1.70 ± 0.10	Q_1 (II)
16148	AX-1329	55.42268	158.59192	1224	1.37 ± 0.02	0.1832 ± 0.0013	56.2	1.93 ± 0.06	
16202	AX-1322	55.42738	158.65350	1946	0.88 ± 0.015	0.244 ± 0.003	81.2	4.0 ± 0.20	
16154	AX-1304	55.37947	158.61380	1281	0.732 ± 0.015	0.226 ± 0.002	47.6	4.4 ± 0.20	N_2 (I)
16153	AX-1340	55.40279	158.56986	1376	1.04 ± 0.02	0.352 ± 0.002	61.1	4.9 ± 0.20	
Kostina Mt. massif									
16283	MILK-0917	55.13255	158.16315	1261	1.84 ± 0.02	0.434 ± 0.002	16.8	3.40 ± 0.08	N_2 (C)
16282	MILK-0903	55.08162	158.22373	862	1.33 ± 0.02	0.320 ± 0.003	47.6	3.47 ± 0.12	
–	Z-142	55.15272	158.22576	980*	–	–	–	4.90 ± 0.20	
21	MILK-0914	55.12041	158.25803	1213	0.59 ± 0.005	0.0656 ± 0.003	67.0	5.10 ± 0.08	$N_{1/2}$ (B)
20	MILK-0913	55.12224	158.25807	1182	0.65 ± 0.005	0.079 ± 0.004	71.4	5.59 ± 0.30	
19	MILK-0911	55.12475	158.25435	1022*	0.87 ± 0.005	0.107 ± 0.005	60.0	5.63 ± 0.09	
65	MILK-0912	55.12325	158.25569	1079	0.50 ± 0.005	0.0874 ± 0.006	83.5	8.00 ± 0.35	N_1 (A)
Uglovoy stream									
64	MILK-0909	55.12607	158.23836	728	0.94± 0.006	0.513±0.004	41.8	24.9 ± 0.90	Pg

Note. K-Ar dating was made in IGEM RAS (samples 16147-16203) and GIN RAS (19-21, 64, 65). Sample Z-142 – after (Khasanov et al., 2009).
(–) – no data. * collapse.

a relatively small lava center (1751.3 m) at the SW slope of the Akhtang stratovolcano (Fig. 2).

The third stage of activization (stage III, Q_2), in the middle Pleistocene (0.3–0.2 Ma, Table 1) started after the quiescence period which lasted about 1.5 m.y. During this stage numerous monogenetic centers, forming several chains crossing the massif to the NE, were formed. Also, a third, SW summit of the massif was formed (1655.9 m). Probably the Q_2 stage also consisted from two or even three successive episodes, when substantially lava or scoria edifices were formed.

According to the results of the tephrochronological investigations, there is no Holocene volcanism within the Akhtang massif (Pevzner, 2015).

On the basis of the obtained isotopic and petrological-geochemical data, we compiled a revised geological map of the Akhtang massif (Fig. 2).

Kostina Mt. massif. We include three relatively isolated but closely located morphological edifices in this massif (Fig. 3*a*): (1) Zagadka Mountain (1583.1 m) which is a large fragment (10 × 15 km) of the substantially destroyed volcanic edifice; most of it is represented by lava ridges with rather steep slopes (Fig. 3*b*). Best preservation is typical for the southern flanks, where significant areas of plateau-effusives have been preserved (Fig. 3*a*). The surface of these plateaus is free from the primary volcanic relief and is gently sloped to the south. Lavas, located at heights more than 1300 m, bear traces of glacial processes. There are many large collapses of different age at the foot of the mountain, most likely together with the old moraines. (2) Kubinskaya Mountain (1229 m) is a small residue of the plateau (3 × 5 km) elongated from the NW to the SE. Perhaps it is a fragment of some substantially destroyed monogenetic center. The southwestern slope of the mountain is rather steep, produced probably by the large collapse. Other sectors are characterized by the successive decrease of the upper parts of lava flows from the main summit to the NW, NNE, SE. Fragments of the lava ridges diverge fan-like from the summit to the NE; these are the remnants of the primary volcanic relief. (3) Kostina Mountain (1752.5 m) – the main summit of this massif – is a large (no less than 13 km across) strongly eroded volcano, composed mainly by lavas. Its top is perfectly readable in relief – sharp lava ridges with steep cliffs diverge from it. Collapse circuses are filled by the deposits of rockfalls and moraines of different ages. Lavas of the last stage of activity are best preserved in the NE and SE sectors of the edifice and are traced minimum at 6–7 km from the summit. Preserved fragments of the upper lava layers at altitudes more than 1300 m have steep slopes, their surface is marked with longitudinal grooves which may be interpreted as traces of the glacier exaration work. Mostly remote lavas of the SE sector form a plateau-like surface at 1200–1300 m altitude; morphologically it is the same at Kubinskaya Mt. or Zagadka Mt. plateaus.

To determine the isotopic age of the plateau-effusives we sampled a lava cross-section of Zagadka Mt. plateau (Fig. 3*b*), and top lava flows of Kostina and Kubinskaya Mts. Also we tried to estimate the age of the rocks from the massif's basement. A series of K-Ar dates was obtained for this collection (Table 1).

The lava of the subvolcanic body in the valley of Uglovoy stream, which is part of the massif's basement, was formed in the late Oligocene about 25 Ma. Having only one dated sample, we are not ready to make interpretations of the early stages of the SR volcanic belt formation.

For the effusive rocks, the oldest ages were received for Zagadka Mt. lavas (8.0–5.1 Ma). Khasanov et al. (2009) published a K-Ar age definition of 4.9 ± 0.2 for the western slope of this mountain (the collapse from the upper part of

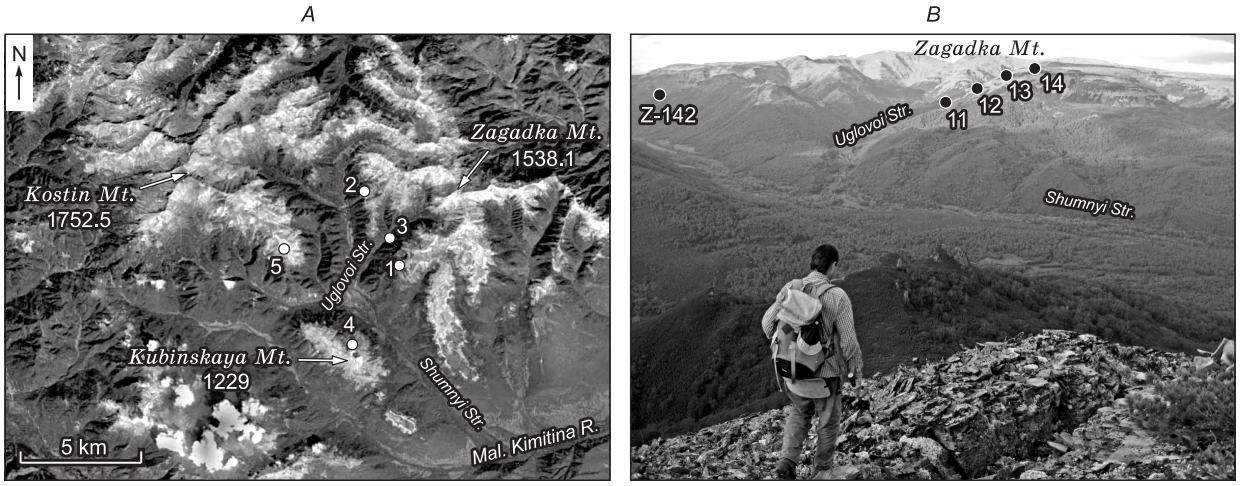

Fig. 3. Kostina Mt. massif. A, location of the objects of this study: 1–5, sampling sites of the rocks for the isotopic dating: 1–2, Zagadka Mt. lavas: 1, samples MILK-0911, -12, -13, -14, 2, sample Z-142 after (Khasanov et al., 2009); 3, subvolcanic body in the Uglovoy stream valley, sample MILK-0909; 4–5, top lava flows: 4, Kubinskaya Mt. (MILK-0903), 5, Kostina Mt. (MILK-0917). B, view to Zagadka Mt. from the SW from the top of Kubinskaya Mt. Photo courtesy Maria Tolstykh. Dots indicate sampling sites (MILK-0911, -12, -13, -14 and Z-142) for the isotopic dating (see Table 1).

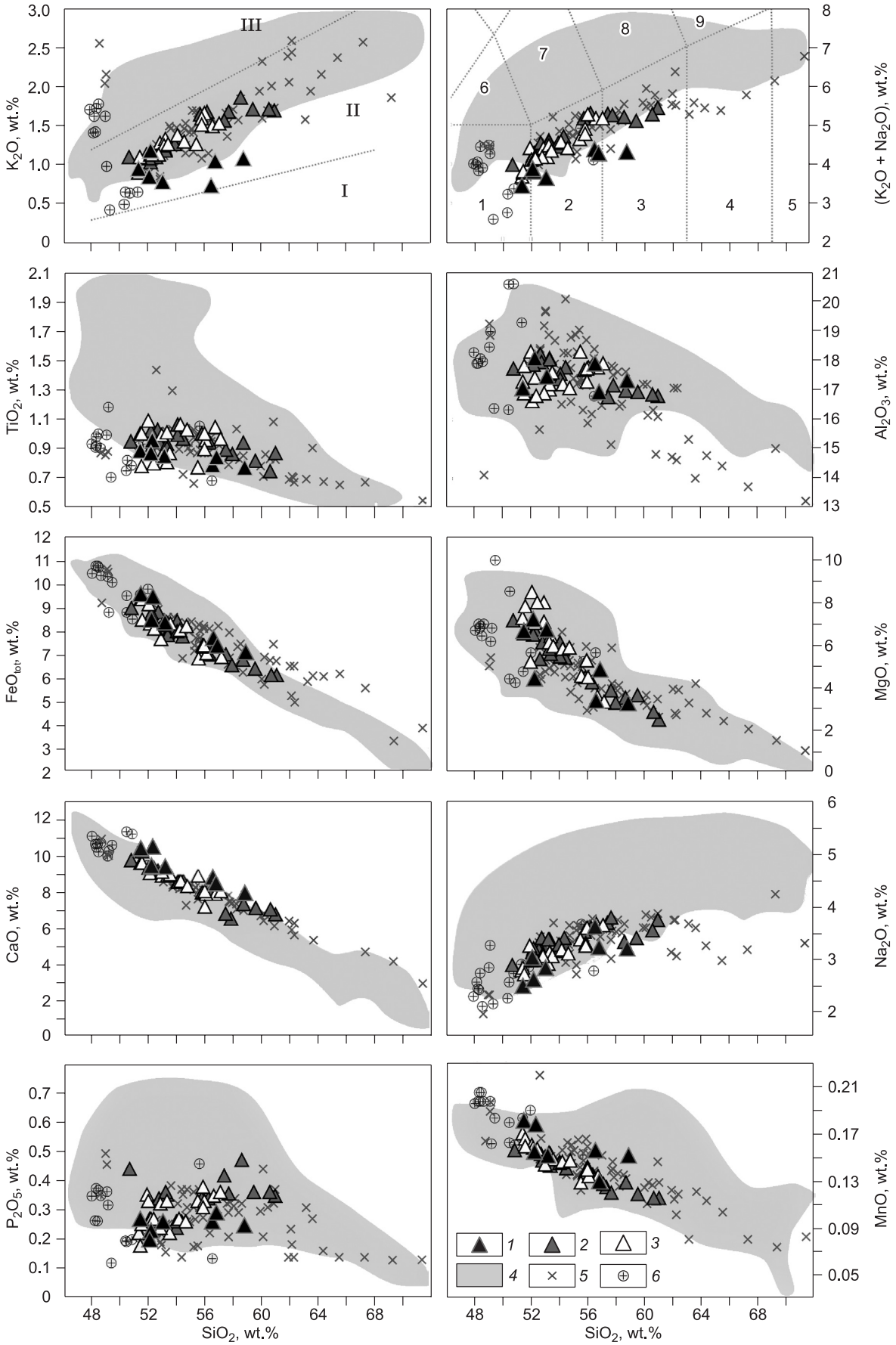
K2O, wt.%
III
II
I
(K2O + Na2O), wt.%
1
2
3
4
5
6
7
8
9
TiO2, wt.%
Al2O3, wt.%
FeOtot, wt.%
MgO, wt.%
CaO, wt.%
Na2O, wt.%
P2O5, wt.%
MnO, wt.%
SiO2, wt.%
SiO2, wt.%
1
2
3
4
5
6

Fig. 4. Harker diagrams for the volcanic rocks of Akhtang massif. Discrimination lines at diagrams a) and b) after (Le Maitre, 1989); fields, (a): I, low-K rocks; II, medium-K rocks; III, high-K rocks; (b): 1, basalts; 2, basaltic andesites; 3, andesites; 4, dacites; 5, rhyodacites; 6, trachybasalts; 7, basaltic trachyandesites; 8, trachyandesites; 9, trachydacites. Legend, rocks: 1–3, of the three stages of volcanic activization: 1, stage I (4.9–4 Ma); 2, stage II (1.9–1.7 Ma); 3, stage III (0.3–0.2 Ma); 4, "western" flank of the southern part of the SR (Volynets et al., 2018 and unpublished author's data) and Quaternary rocks of the northern part of the SR (Volynets et al., 2010); 5, "eastern" flank of the southern part of the SR (except Akhtang and Kostina Mt. massifs) and Anaunsky Dol (Volynets et al., 2018 and unpublished author's data); 6, Neogene rocks of the northern part of the SR (Volynets et al., 2010).

the plateau), which is in good agreement with our data on the early Pliocene age of the lavas from the top of Zagadka Mt. It is notable that there is a quiescence period about 2.4 m.y., which divides effusives with 8 and 5 Ma ages. Our data also allow us to estimate the duration of the volcanism activization phase at the Miocene-Pliocene boundary as about 0.7 m.y.

Close age definitions were received for the top lava flows of Kubinskaya Mt. (3.47 ± 0.12 Ma) and Kostina Mt. (3.40 ± 0.08 Ma). These volcanic centers belong to the late Pliocene stage of the activity of this massif (Table 1). The duration of the period of rest dividing the early and late Pliocene stages, is about 1.4 m.y. It is notable that the younger centers of Kostina Mt. massif (Kubinskaya Mt. and Kostina Mt.) are located to the west from the older center (Zagadka Mt.).

Therefore for the Kostina Mt. massif we also can distinguish three stages of volcanic activity, which are divided by the long quiescence periods: A – late Miocene (N_1), B – Miocene-Pliocene boundary ($N_{1/2}$), and C – late Pliocene (N_2).

Geochemistry of volcanic rocks. *Akhtang massif.* All analyzed volcanic rocks belong to the medium-K calc-alkaline series and are represented by basalts to andesites. All rocks of the massif are similar to the previously studied lavas from the "eastern" flank of the southern part of the SR (Volynets et al., 2018). In comparison with the rocks of the "western" flank and the Quaternary lavas of the northern part of the SR, they have lower TiO_2, K_2O, Na_2O, P_2O_5 and slightly higher CaO (Fig. 4) and Mg#. Rocks of all three stages of activization are similar by their major element content, although most lavas of the Pliocene stage (I) have decreased K_2O concentrations and higher Na_2O/K_2O than Quaternary rocks (stages II and III). Rocks of Stage I are divide to two groups by major element content. Plateau-effusives of the early phase have more acid compositions and are represented by basaltic andesites and andesites (SiO_2 55.81– 58.11 wt.%), while Akhtang stratovolcano lavas, formed during the final phase of the Pliocene stage, are basalts – basaltic andesites (SiO_2 50.7 – 52.38 wt.%).

Early Pleistocene rocks (Stage II) are slightly more alkaline and are characterized by the maximal variations of silica content among all studied rocks of the Akhtang massif, while the youngest, middle Pleistocene (Stage III) basalts and basaltic andesites have the highest Mg#. Nevertheless, all described variations are moderate and with rare exceptions can be combined into the same fractionation trends (Fig. 4).

Microelement composition was measured in a series of representative samples. Pliocene rocks (Fig. 5*A*) are characterized by the island arc type of microelement distribution: substantially depleted Nb, Ta, Hf, Zr and REE and elevated LILE/HFSE ratios. Basaltic andesites and andesites have slightly increased REE content compared to basalts of the same stage, with difference in HREE concentrations more pronounced in comparison with LREE. All volcanic rocks of Stage I – both of the early (plateau) and late (stratovolcano) phases are similar to the Neogene plateau-effusives of the SR in their microelement distribution (Fig. 5*A*) (Volynets et al., 2010, 2018).

The next two stages (early and middle Pleistocene) have the largest variations in microelements contents. Here we found both island arc and hybrid type varieties with increased HFSE concentrations (Fig. 5*B, C*). Among the early Pleistocene lavas (Stage II) the most enriched spectra of the incompatible elements with Nb up to 8.5 and Ta up to 0.52 ppm are typical for andesites. Basalts of the same stage are close in composition to Pliocene rocks but differ from them in a little bit higher concentrations of Nb and Ta (2.4 and 0.12 vs. 1.5 and 0.09 ppm, respectively).

Lavas of the Middle Pleistocene (Stage III) (Fig. 5*C*) also have variable concentrations of microelements. There are two types of basalts. The first type has island arc type patterns with low HFSE and high LILE concentrations; composition of these rocks is similar to those of Stage I. The second type of basalts has hybrid type of microelement distribution with a low degree of enrichment (Nb ~ 5 ppm, Ta ~ 0.3 ppm). Basaltic andesites of Stage III also are more enriched compared to the less fractionated varieties. Most evolved lavas of the shield-like monogenetic center at the SW sector of the massif (h = 1140.2, Fig. 2) contain 56.56 wt.% of SiO_2 and 7.9 ppm Nb. Positive correlations of Nb, Ta, Hf, Zr with SiO_2, K_2O and negative with Mg#, Ni are observed for the early and middle Pleistocene rocks (while there are no such correlations for the Pliocene rocks)

Kostina Mt. massif. All studied rocks belong to the medium-K calc-alkaline series and are represented by basalts to andesites with predominant basaltic andesites (Fig. 6). Lavas of the stages A (N_1) and B ($N_{1/2}$) have lower concentrations of K_2O, Na_2O, TiO_2, P_2O_5 than the rocks of the upper structural horizon, belonging to the late Pliocene, while MgO and CaO concentrations are, on the contrary, higher (concentrations of MgO in Zagadka Mt. lavas (stage A (N_1)) are the highest of all previously studied rocks of the "eastern" flank of the southern part of the SR). In general, the composition of rocks from this area is similar to that of the previously studied rocks of the "eastern" flank of the southern part of the SR, with exception of even lower concentrations of TiO_2 and P_2O_5 in N_{1-2} lavas (stages A and B). A critical difference is observed in concentrations of micro-

elements of the three stages (Fig. 7). Plateau-effusives of the stages A and B (8–5 Ma) have typical island arc characteristics: high LILE/HFSE, pronounced Nb-Ta minimum, low HFSE content. Lavas of the upper structural horizon (top parts of Kubinskaya and Kostina Mts.), for which we received isotopic age definitions ~3.5 Ma (stage C, N_2) are characterized by the hybrid type of microelement distribution with higher La/Yb, Ta/Yb, Nb/Y, Dy/Yb, Ce/Pb and lower LILE/HFSE compared to the rocks of the first two stages (Fig. 7). The $N_{1/2}$ plateau-effusives of Kostina Mt. massif are similar in microelement composition to the rocks of the N_2 (I) stage of the Akhtang massif, while hybrid N_2 (C) lavas of this area are similar to the rocks of the Akhtang's Q_2 (III) stage (superimposed zone of monogenetic cones at the SW slope of the Akhtang massif).

Isotopic composition of Sr and Nd. For all distinguished stages of activization of the Akhtang and Kostina Mt. massifs we have measured isotopic composition of Sr and Nd in the representative samples (Supplementary material (http://sibran.ru/journals/supp_mateirals.xlsx) and Fig. 8). Lavas of the Akhtang massif demonstrate a rather stable Nd isotopic composition (0.513060–0.513065) and slightly more pronounced variations of Sr isotopes (0.703350–0.703423). Previously published data on the Akhtang massif (Churikova et al., 2001) (for three samples of lavas from monogenetic cones of the SW sector of the volcano) have shown a bit lower $^{143}Nd/^{144}Nd$ at similar $^{87}Sr/^{86}Sr$; these samples also have higher Ta/Yb, Nb/Y, Ce/Pb ratios. Volcanic rocks from the Kostina Mt. massif show more substantial variations of isotopic ratios (Supplementary material and Fig. 8). With the exception of two samples, Sr isotopes of the rocks from this massif are similar to those of Akhtang at higher $^{143}Nd/^{144}Nd$. The high-Mg lava of the stage A (N_1) has most primitive Sr and Nd isotopic ratios, while andesite of the stage C on the contrary has increased $^{87}Sr/^{86}Sr$ and $^{143}Nd/^{144}Nd$ ratios; these two samples occupy separate positions in the $^{87}Sr/^{86}Sr$ vs. $^{143}Nd/^{144}Nd$ diagram.

DISCUSSION

Centers of plateau-effusives eruptions in the Sredinny Range. Until now, it is not well understood, where were the centers of plateau-effusives eruptions, and what was the mechanism of their formation, although they are widespread along the main watershed of the SR. The centers are either destroyed or overlain by younger volcanic rocks. Thus, for example, in the case of the early Pliocene plateaus of the Akhtang massif or lavas of Zagadka Mt., there are pretty large, but still, only fragments of the substantially eroded volcanic edifices. Our geochemical and isotopic study of the Akhtang massif enabled us to demonstrate the similar age and chemical composition of rocks which form the upper part of the stratovolcano and plateau-effusives of its basement. Although is it unlikely that the stratovolcano edifice

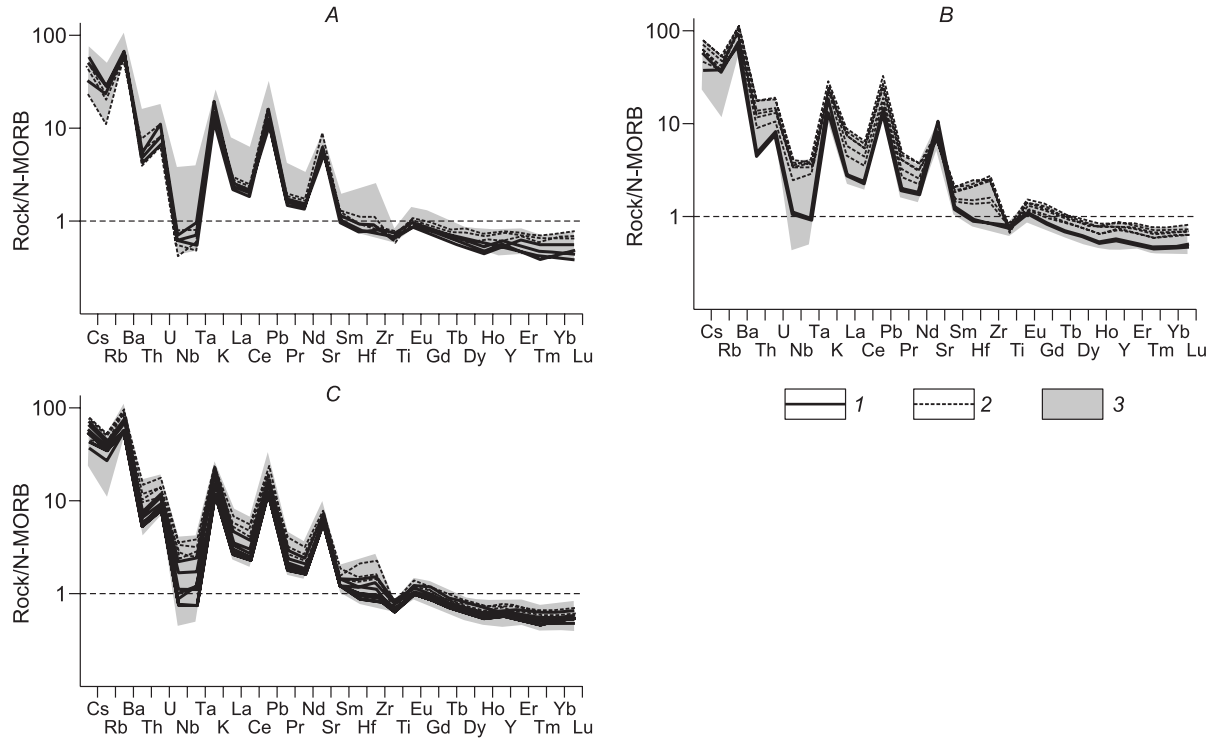

Fig. 5. N-MORB-normalized trace element distributions for rocks of the three stages of volcanic activization of Akhtang massif. Compositions: 1, basalts and basaltic andesites with SiO_2 < 54 wt.%; 2, basaltic andesites with SiO_2 > 54 wt.% and andesites; 3, all analyzed rocks of the Akhtang massif. Stages of volcanic activization: a) I (N_2); b) II (Q_1); c) III (Q_2). Composition of N-MORB after (Sun and McDonough, 1989).

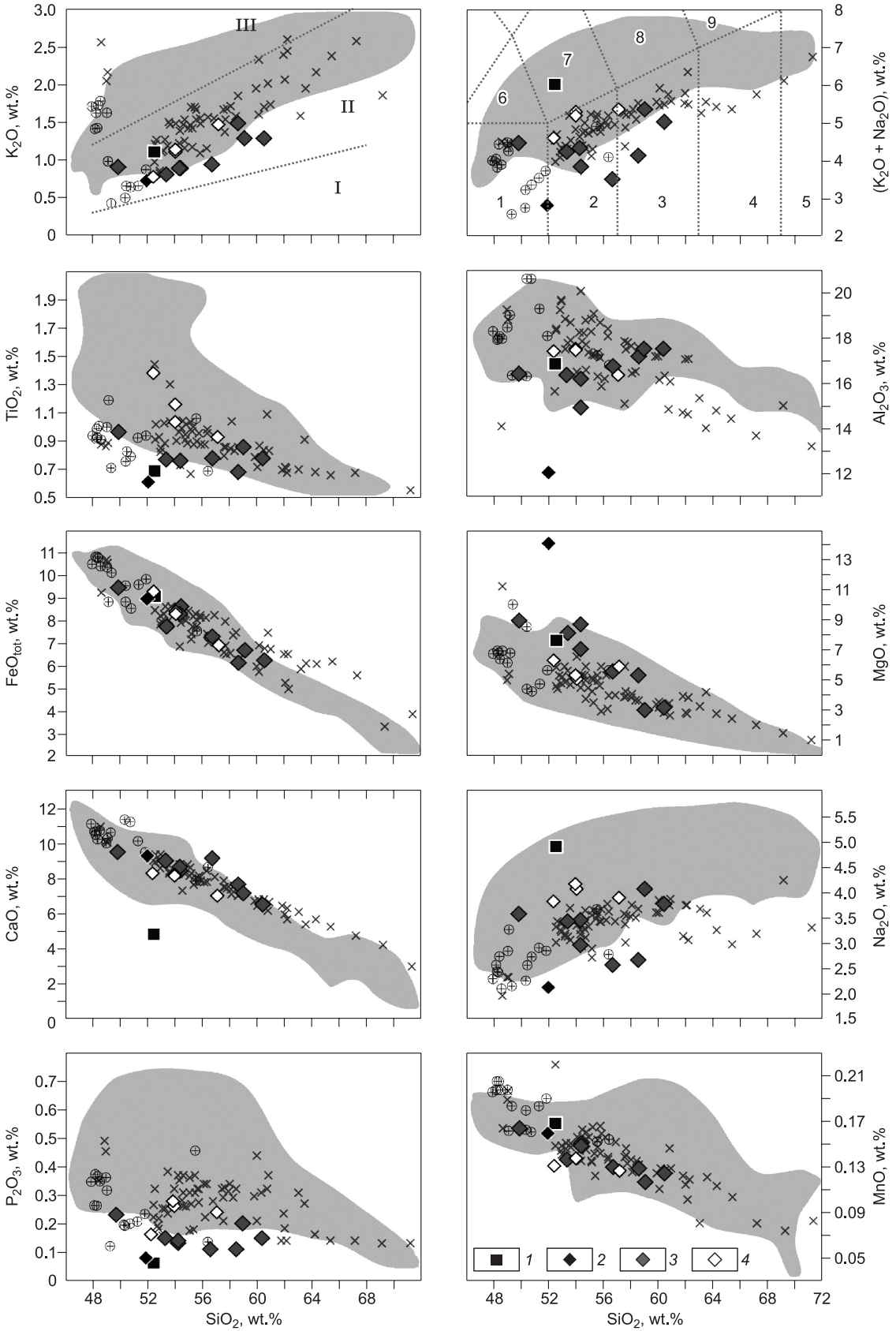

Fig. 6. Harker diagrams for the volcanic rocks of the Kostina Mt. massif. Discrimination lines at diagrams a) and b) after (Le Maitre, 1989). Legend, rocks: 1, lava of Uglovoy stream (25 Ma); 2, stage A (8 Ma); 3, stage B (5.6 – 4.9 Ma); 4, stage C (~ 3.5 Ma); other symbols are the same as 4–6 at Fig. 4.

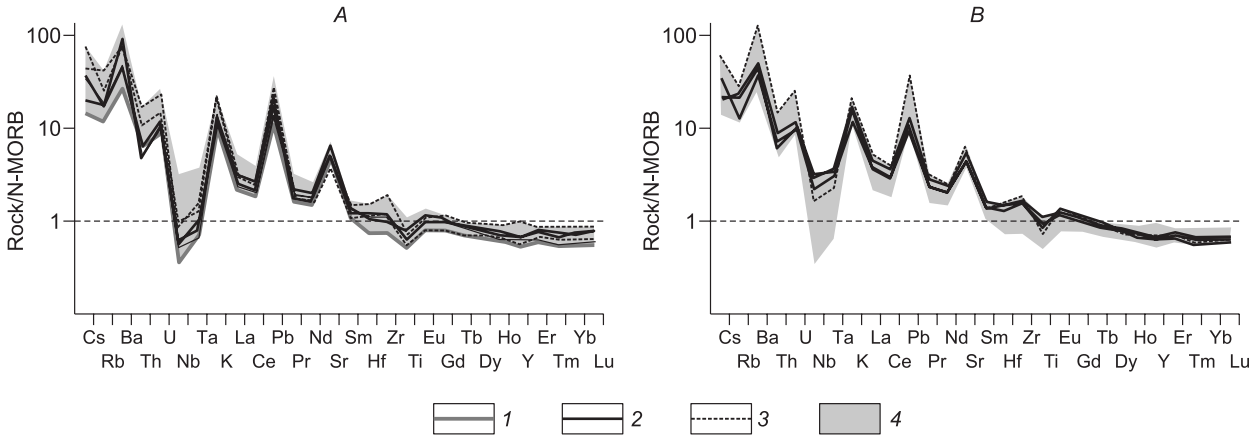

Fig. 7. N-MORB-normalized trace element distributions for rocks of the three stages of volcanic activization of the Kostina Mt. massif. Compositions: 1–2, basalts and basaltic andesites with SiO_2 < 54 wt.%; 3, basaltic andesites with SiO_2 > 54 wt.% and andesites; 4, all analyzed rocks of Kostina Mt. massif. *A*, lavas of stage A (1) and B (2 and 3); *B*, stage C.

was the center of effusion of plateau (due to its superimposed character), we can suppose the same source of magmatic feeding of these eruptions. Age definitions made for the Kostina Mt. massif also argue for the hypothesis that plateau-like surfaces could have been formed during substantially effusive eruptions of the central type.

Isotopic age of volcanic rocks and periods of activization and quiescence. Our research on isotopic dating of volcanic rocks revealed that in the Akhtang massif during the last 5 m.y. there were at least three bursts of volcanic activity, separated by long repose periods. The first stage of activization consisted of two phases. The early, and, apparently, main phase for this stage was marked by the effusion of the spacious lava flows with plateau-like morphology, while during the late phase, a stratovolcano edifice was formed. The composition of rocks varies from andesites and basaltic andesites (plateau) to basalts (stratovolcano) of the island arc type. During the second stage, the activity was concentrated in the NW sector of the massif. A large lava volcano with acid composition of rocks was formed at the beginning of this stage, and later a small lava center grew at the SW foot of the Akhtang stratovolcano. Andesites of the early phase of Stage II bear evidence of the extensive fractionation in the open system, which is manifested by the increase of incompatible elements concentrations correlated with the increase of silica content; elevated HFSE concentrations in these rocks are most likely not connected to the composition of the mantle source. At the same time, geochemical features of the basalts of the late phase of Stage II are similar to those of the volcanic rocks of Stage I. All rocks have subduction signatures. The third, middle Pleistocene stage is marked by the development of the monogenetic volcanism, associated with the NE faults. During this stage, both island arc and hybrid type rocks with low enrichment degree were erupted.

On the example of the Akhtang massif we show, for the first time, that quiescence periods may have reached 1.5–2 m.y., and the resumption of the volcanic activity was accompanied by change in both composition of rocks and type of activity (plateau-effusives – stratovolcano – lava volcano – monogenetic centers). The indicated stages of activization correlate with the regional episodes of increasing volcanic activity in the NW Pacific (Prueher and Rea, 2001); the middle Pleistocene stage turned out to be synchronous to the activization episode which led to the formation of the Klyuchevskaya group of volcanoes (Calkins, 2004; Churikova et al., 2015), as the well as formation of numerous monogenetic centers in eastern Kamchatka (Nishizawa et al., 2017).

It is interesting that in the Akhtang massif, for the largest chains of sub-simultaneous monogenetic centers of Stage III, we observe successive increase of the SiO_2 content from the more southern to the more northern eruptive centers (Supplementary material):

(1) KAR-1301 (51.4) → KAR-1304 (52.13) → KAR-1303 (53.1) → KAR-1306 (53.4) → AX-1351 (55.4 wt.%),

(2) AX-1350 (51.9) → AX-1346 (51.95) → AX-1342 (52.8) → AX-1343 (53.2 wt.%).

An analogous pattern was previously found for Holocene eruptions of scoria cones in the SR (Pevzner, 2015).

A similar evolution of magma generation processes is observed also within the Kostina Mt. massif, which is located to the south of Akhtang. Here we also documented three stages of volcanism activization, which are separated by the long (1.4 and 2.4 m.y.) periods of rest. It is notable that two early stages (A and B) are characterized by the effusions of ultimately island arc type lavas. At the late stage (C) hybrid type basaltic andesites appeared, which are similar to the hybrid rocks with low enrichment degree, described earlier in the Ichinsky and Alney massifs (Churikova et al., 2001; Volynets et al., 2010). It is interesting that the centers of hybrid lavas eruptions (Kostina and Kubinskaya Mts.) are located several km to the west compared to the main eruptive center – Zagadka Mt. (i.e. the distance from the supposed position of the Miocene subduction trench increased).

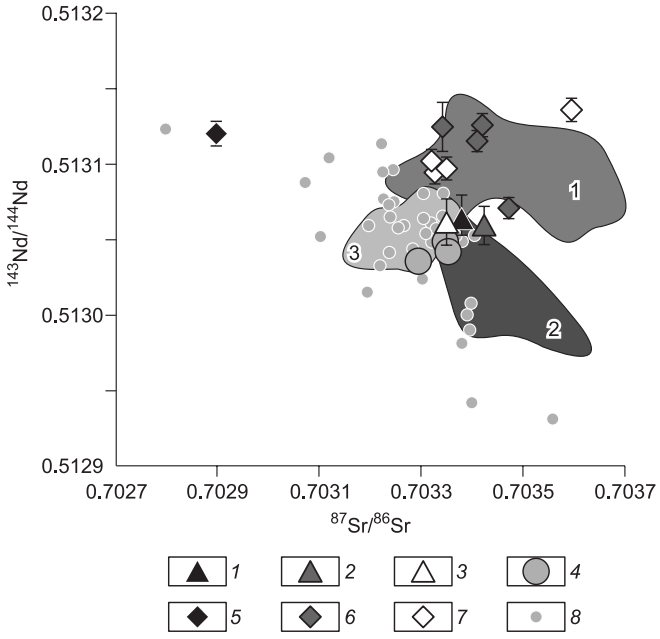

Fig. 8. Sr and Nd isotopic composition in the representative samples of the Akhtang and Kostina Mt. massifs compared to the previously studied rocks of other volcanic centers of Kamchatka. Legend, rocks: 1–4: Akhtang massif, 1–3, our data: 1, Stage I; 2, Stage II; 3, Stage III; 4, after (Churikova et al., 2001); 5–7: the Kostina Mt. massif, 5, stage A (N_1); 6, stage B ($N_{1/2}$); 7, stage C (N_2); 8, previously studied rocks of the SR, after (Churikova et al., 2001; Volynets et al., 2010; Koloskov et al., 2013). Numbered fields correspond to the composition of rocks from: 1, Central Kamchatka Depression (Klyuchevskoy and Tolbachik), after (Churikova et al., 2001; Portnyagin et al., 2007; Portnyagin et al., 2015); 2, Eastern volcanic belt (Kizimen, Gamchen, Shmidt) after (Churikova et al., 2001); 3, Southern Kamchatka (Mutnovsky and Gorely) after (Duggen et al., 2007).

Therefore, there are three stages of activization, distinguished for both massifs. Two early stages in both cases are characterized by island arc type lavas. Early stages of both the Akhtang massif (early phase of Stage I (plateau) and Stage II) and Kostina Mt. massif (stages A and B) are separated by the similarly long repose period of 2.4 m.y. The third, final stage of activization in both massifs is documented after a period of rest of 1.4 m.y. Hybrid type rocks for the first time appear during the third stage in both massifs.

The Kostina Mt. massif is studied in less detail than the Akhtang massif. It is very likely that after additional work on isotopic dating we can find lavas of the "late" phase of stage A with an age about 7.7 Ma, in which case we will reach an absolute identity of the repose periods. But even with the available data, we can argue for the common regional causes which trigger outbreaks of volcanism at the SE flank of the southern part of the Sredinny Range of Kamchatka.

Magma sources. The established age frame of the volcanic activity within the Akhtang massif exclude the possibility that all magmas were formed by fractionation of a common parent melt, despite the similarity of the composition of the studied rocks. Indeed, it is hard to imagine a magma reservoir, which could possibly exist in a melted state during almost 5 m.y., with repose periods up to 2 m.y. Therefore, the close geochemical composition of the volcanic rocks is most likely caused by the similar composition of the melted matter. Positive correlations of Nb, Ta, Zr concentrations with the fractionation factors (Ni, MgO, Mg#, etc.) in the rocks from stages II and III allow to suggest that increased HFSE concentrations in basaltic andesites and andesites of Stage II and in basaltic andesites of monogenetic centers are not inherited from the primary magmas but were acquired during the open-system evolution of the magmas (Lee et al., 2014; Portnyagin et al., 2015) or/and due to crustal contamination processes. Therefore, in our discussion on the composition of the source, we limit the selection by the more basic rocks with $SiO_2 < 54$ wt.% and MgO > 6 wt.%. As it is clear from Fig. 5, microelement distribution patterns contradict the idea of the pure fractionation-derived chemical variations of the rocks composition, but imply heterogeneity of the mantle and fluid sources, involved in magma genesis in the Sredinny Range. The position of this massif in the frontal zone of the Oligocene–Miocene subduction zone likely caused substantial metasomatism of the mantle wedge by the fluid. That caused not only high, typically island arc LILE/HFSE ratios in Neogene rocks, but also increased these values in the Quaternary rocks, when the Pacific trench already moved to the east, and the massif itself was in the back-arc part of the system, 300 km above the upper part of the slab. Participation of the enriched mantle is observed only in part of the samples and weakly expressed. At the same time, sub-simultaneous eruptions of the typical island arc and hybrid magmas within the limited area bear evidence of the possible variability of the depth of magma generation and of the heterogeneous composition of the mantle. Isotopic characteristics of the studied rocks of all three stages indicate a depleted mantle source similar to MORB with fluid addition, which is expressed by the increased Sr isotopic ratios relative to MORB. Those rocks which have slightly decreased Nd isotopic ratios also have slightly increased Ta/Yb, Nb/Y. This may be a result of the metasomatized sublithospheric mantle participation in the genesis of these rocks (Turner et al., 2017; Volynets et al., 2018). As is has been demonstrated in a series of publications (e.g., O'Reilly and Griffin, 2013), the sublithospheric mantle is highly heterogeneous (on a scale from microns to terrains) and bears record of numerous episodes of fluids/melts interaction with its domains. Obviously, the composition of melts which produced the monogenetic cones of the Akhtang massif (Stage III) is dependent on the composition of the mantle domain which was melted Turner et al. (2017) argue that when continental crust blocks are present in the back-arc zone of an island arc system, the enriched lithospheric mantle domains may be eroded to the asthenosphere and participate in melting in the back-arc, revealing themselves by the increased HFSE concentrations, characteristic isotopic ratios and elemental ratios. But, obviously, if only the depleted mantle wedge reworked by subduction fluid is involved

in melting, the composition of the resulting melt will be typical island arc without any records of the enriched material participation. In the Quaternary, due to the subduction front migration to the east and therefore change of the geodynamic setting in the Sredinny Range, the fluid flow here became less intensive, and the melting degree decreased. The final stage of the Akhtang massif evolution is a monogenetic volcanism stage. Turner et al. (2017) argued that namely small eruptive centers may tap mantle sources with a larger component of decompression, and so tend to produce melts that are enriched in EM1-like components (the presence of which in the back-arcs is considered by the authors as a result of interaction with sublithospheric metasomatised mantle). This is in full agreement with our observations (Volynets et al., 2018).

Geochemical features of the Kostina Mt. massif may serve as a model for demonstration of the change of the source characteristics due to the altered geodynamic setting in the Sredinny Range. During the Miocene and the early Pliocene typical island-arc rocks were formed; they have high LILE/HFSE, low HFSE and REE concentrations, which are not correlated to the silica content. Sr isotopic ratios are similar to those of the Akhtang rocks, which points to the close compositions of the mantle and fluid sources of these magmas. After the ~1.5 m.y. repose period, volcanic activity within this massif resumed somewhat westwards and was accompanied by a change in rocks geochemistry to the hybrid type with HFSE increase and sharp decrease of LILE/HFSE ratios. For these rocks, we also observe slightly lessened $^{143}Nd/^{144}Nd$, which enables us to argue for the same mechanism of their generation, which we proposed for the hybrid rocks of the Akhtang massif.

CONCLUSIONS

1. For the first time we report geochemical and isotopic data characterizing the evolution of the Akhtang and Kostina Mt. massifs during the late Miocene–Quaternary. We show that during the Miocene–early Pliocene (the Kostina Mt. massif) and in the Pliocene (the Akhtang massif) basalts and basaltic andesites with island arc type of microelement distribution prevail. The final stage of volcanism within both massifs is marked by the hybrid type rocks eruptions; the degree of their enrichment is low.

2. We prove the sub-simultaneity and principal geochemical similarity of the rocks which build the upper part of the Akhtang stratovolcano and of plateau-effusives from its basement. Dating of rocks of the Kostina Mt. massif also allow us to propose that plateau-like surfaces might have been formed during effusive eruptions of the central type.

3. According to the results of the firstly conducted K-Ar dating we determined three stages of the Akhtang massif activization: 4.9–4.0, 1.9–1.7 and 0.3–0.2 Ma; and three stages of the Kostina Mt. massif activization: ~8, 5.6–4.9 and ~3.5 Ma. For two early stages of both massifs, island arc rocks are typical, while during the third stage, rocks of the hybrid geochemical type appear.

4. On the example of the Akhtang and Kostina Mt. massifs we report for the first time the existence of long (1.4–2.4 m.y.) quiescence periods in volcanic activity. After them, the character of eruptive activity (in the Akhtang massif, from plateau-effusive eruptions to stratovolcano and monogenetic volcanism) and composition of the magma sources changed. The indicated stages of activization of the Akhtang massif correlate with some episodes (about 4.9, 4.0, 1.9–1.7, 0.3–0.2 Ma) of the increasing volcanic activity in the NW Pacific, registered in the DDP 882 and 887 in Kamchatka and Aleutians water area (Prueher and Rea, 2001); the middle Pleistocene stage is synchronous with the activization episode which led to the Klyuchevskaya group of volcanoes formation (Calkins, 2004; Churikova et al., 2015), as well as with the formation of the numerous monogenetic centers in Eastern Kamchatka (Nishizawa et al., 2017).

5. In the middle Pleistocene, a series of faults crossed the Akhtang massif predominantly in the NE direction. Monogenetic centers are associated with these faults. Within the Kostina Mt. massif, monogenetic volcanism is not found. Nevertheless, to the north along the "eastern" flank there are plenty of well preserved monogenetic cones (i.e., their age is presumably middle to late Pleistocene); some of these edifices even have proved Holocene age (scoria cones and lava flows of the Kirevna and the Levaya Belaya rivers in the Alney-Chashakondzha massif (Pevzner, 2015)). Available data on the composition of volcanic rocks of monogenetic centers of the Alney-Chashakondzha massif show their principal similarity with the lavas of the final stages of the Akhtang and Kostina Mt. massifs and allow us to argue for the common magma generation mechanism within the whole "eastern" flank of the southern part of the Sredinny Range of Kamchatka during the Pliocene-Quaternary.

This work is performed in accordance with the research theme of IVS FEB RAS 0282-2019-0009 (data analyses) and GIN RAS № 0135-2019-0059 (geochronological research) and with financial support from RFBR grant № 17-05-00112 (analytical work). Detailed reviews made by Dr. A.B. Perepelov and Dr. Yu.A. Martynov helped us to improve the earlier version of this manuscript. Authors are grateful to Vladimir Rodin and Boris Tagirov for the help and collaboration during the field works, to Georgy Ovsyannikov for the sample preparation, to Vasily Karandashev and Anton Yakushev for the analytical work.

REFERENCES

Avdeiko, G.P., Palueva, A.A., 2009. Geodynamic of the Kamchatka subduction zone: volcanism, seismic danger, tsunami danger, in: Volcanism and Geodynamic: IV Russian Symposia on Volcanology and Paleovolcanology [in Russian]. IVS FEB RAS, Petropavlovsk-Kamchatsky. Vol. 1, pp. 567–570.

Avdeiko, G.P., Popruzhenko, S.V., Palueva, A.A., 2002. Tectonic evolution and volcano-tectonic zoning of Kurile-Kamchatka island-arc system. Geotectonika, No. 4, 64–80.

Avdeiko, G.P., Palueva, A.A., Khleborodova, O.A., 2006. Geodynamic conditions of volcanism and magma formation in the Kurile-Kamchatka island-arc system. Petrology 14 (3), 230–246.

Calkins, J., 2004. $^{40}Ar/^{39}Ar$ geochronology of Khapitsa Plateau and Studyonaya River basalts and basaltic andesites in Central Kamchatka Depression, Kamchatka, Russia. Abstr. IV JKASP Int. workshop. http://www.kscnet.ru/ivs/conferences/kasp/tez/ab21en.doc

Chernyshev, I.V., Bakharev, A.G., Bortnikov, N.S., Goltsman, Y.V., Kotov, A.B., Gamyanin, G.N., Chugaev, A.V., Sal'nikova, E.B., Bairova, E.D., 2012. Geochronology of igneous rocks at and near to the Nezhdaninka gold deposit, Yakutia, Russia: U-Pb, Rb-Sr, and Sm-Nd isotopic data. Geol. Ore Deposits 54 (6), 411–433.

Churikova, T., Dorendorf, F., Wörner, G., 2001. Sources and fluids in the mantle wedge below Kamchatka, evidence from across-arc geochemical variation. J. Petrol. 42 (8), 1567–1593.

Churikova, T.G., Gordeychik, B.N., Iwamori, H., Nakamura, H., Ishizuka, O., Nishizawa, T., Haraguchi, S., Miyazaki, T., Vaglarov, B.S., 2015. Petrological and geochemical evolution of the Tolbachik volcanic massif, Kamchatka, Russia. J. Volcanol. Geotherm. Res. 307, 156–181.

Duggen, S., Portnyagin, M., Baker, J., Ulfbeck, D., Hoernle, K., Garbe-Schönberg, D., Grassineau, N., 2007. Drastic shift in lava geochemistry in the volcanic-front to rear-arc region of the Southern Kamchatkan subduction zone: Evidence for the transition from slab surface dehydration to sediment melting. Geochim. Cosmochim. Acta 71 (2), 452–480.

Gorbatov, A., Kostoglodov, V., Suárez, G., Gordeev, E., 1997. Seismicity and structure of the Kamchatka subduction zone. J. Geophys. Res. Solid Earth 102 (B 8), 17883–17898.

Jochum, K.P., Weis, U., Schwager, B., Stoll, B., Wilson, S.A., Haug, G.H., Andreae, M.O., Enzweiler, J., 2016. Reference values following ISO guidelines for frequently requested rock reference materials. Geostand. Geoanal. Res. 40 (3), 333–350.

Karandashev, V.K., Turanov, A.N., Orlova, T.A., Lezhnev, A.E., Nosenko, S.V., Zolotareva, N.I., Moskvitina, I.R., 2008. Use of the inductively coupled plasma mass spectrometry for element analysis of environmental objects. Inorgan. Materials 44, 1491–1500.

Karandashev, V.K., Khvostikov, V.A., Nosenko, S.Yu., Burmii, Zh.P., 2016. Highly enriched stable isotopes in large scale analysis of rocks, soils, subsoils and bottom sediments using inductively coupled plasma mass spectrometry (ICP-MS). Industrial laboratory. Diagnostics of materials, No. 82 (7), 6–15.

Khasanov, Sh.G., Sidorenko, V.I., Borovtsov, A.K., Slyadnev, B.I., Rodnykh, N.A., Nikolaeva, V.I. (Eds.), 2008. State Geological Map of the Russian Federation. Scale 1: 200,000. Second edition. Western-Kamchatka Series. N-57-III (Esso) [in Russian]. VSEGEI, St. Petersburg

Khasanov, Sh.G., Litvinov, A.F., Markovsky, B.A. (Eds.), 2009. State geological map of Russian Federation. 2009. Scale 1: 200,000. Second edition. Khangar series. N-57-IX (Milkovo) [in Russian]. VSEGEI, St. Petersburg. Electronic map. 2015.

Koloskov, A.V., Flerov, G.B., Perepelov, A.B., Melekestsev, I.V., Puzankov, M.Yu., Filosofova, T.M., 2013. The evolutionary stages and petrology of the Kekuknai volcanic massif as reflecting the magmatism in the backarc zone of the Kurile-Kamchatka island arc system. Part II. Petrologic and mineralogical features, petrogenesis model. J. Volcan. Seismol. 7 (2), 145–169.

Konstantinovskaya, E.A., 1999. Geodynamics of an island-arc–continent collision in the western part of the Pacific Ocean. Geotektonika, No. 5, 15–34.

Lebedev, V.A., Chernyshov, I.V., Chugaev, A.V., Gol'tsman, Yu.V., Bairova, E.D., 2010. Geochronology of eruptions and parental magma sources of Elbrus Volcano, the Greater Caucasus: K-Ar and Sr-Nd-Pb isotope data. Geochem. Int. 48 (1), 41–67.

Lee, C.-T.A., Lee, T.C., Wu, C.-T., 2014. Modeling the compositional evolution of recharging, evacuating, and fractionating (REFC) magma chambers: Implications for differentiation of arc magmas. Geochim. Cosmochim. Acta 143, 8–22.

Legler, V.A., 1977. Cenozoic evolution of Kamchatka according to plate tectonics theory, in: Sorokhtin, O.G, Zonenshain, L.P. (Eds.), Plate Tectonics (Energy Sources of Tectonic Processes and Plate Dynamics) [in Russian]. Institute of Oceanology AS USSR, Moscow, pp. 137–169.

Le Maitre, R.W. (Ed.), 1989. A classification of the igneous rocks and glossary of terms. Recommendations of the International Union of Geological Sciences on the systematics of igneous rocks. Blackwell Scientific Publications, Oxford.

Nekrylov, N. A., Plechov, P. Y., Bychkov, K. A., Perepelov, A. B., Puzankov, M. Y., Shur, M. Y., Bazanova, L. I., 2015. Parental melts of the last volcanic pulse in the Sedanka field, Sredinny Range, Kamchatka. Mosk. Univ. Geol. Bull. Vol. 70 (3), 233–239.

Nishizawa, T., Nakamura, H., Churikova, T., Gordeychik, B., Ishizuka, O., Haraguchi, S., Miyazaki, T., Vaglarov, B., Chang, Q., Hamada, M., Kimura, J.-I., Ueki, K., Toyama, C., Nakao, A., Iwamori, H., 2017. Genesis of ultra-high-Ni olivine in high-Mg andesite lava triggered by seamount subduction. Sci. Rep. 7, Article 11515.

Nekrylov, N.A, Plechov, P.Y., Popov, D.V., Shcherbakov, V.D., Danyushevsky, L.V., Dirksen, O.V., 2018. Garnet-pyroxenite-derived end-member magma type in Kamchatka: evidence from composition of olivine and olivine-hosted melt inclusions in Holocene rocks of Kekuknaisky Volcano. Petrology 26 (4), 329–350.

Ogorodov, N.V., Kozhemyaka, N.N., Vazheevskaya, A.A., Ogorodova, A.S., Erlikh, E.N., 1972. Volcanoes and Quaternary volcanism of the Sredinny Range of Kamchatka [in Russian]. Nauka, Moscow.

O'Reilly, S.Y., Griffin, W.L., 2013. Mantle metasomatism, in: Harlov, D.E., Austrheim, H. (Eds.), Metasomatism and the Chemical Transformation of Rock: The Role of Fluids in Terrestrial and Extraterrestrial Processes (Lecture Notes in Earth System Sciences). Springer-Verlag, Berlin, Heidelberg, pp. 471–533.

Perepelov, A.B., 2014. Cenozoic magmatism of Kamchatka at the stages of change of the geodynamic situations. Dr. Sci. Thesis [in Russian]. Vinogradov Institute of Geochemistry SB RAS, Irkutsk.

Perepelov, A.B., Chaschin, A.A., Martynov, Yu.A., 2006. Sredinno-Kamchatskaya zone (Pliocene–Holocene), in: Geodynamic, magmatism and metallogeny of the Russian East [in Russian]. Dalnauka, Vladivostok, Vol. 1, pp. 382–398.

Pevzner, M.M., 2015. Holocene Volcanism of the Sredinny Range of Kamchatka, in: Fedonkin, M.A. (Ed.), Transactions of the Geological Institute [in Russian]. GEOS, Moscow. Vol. 608.

Pevzner, M.M., Volynets, A.O., Lebedev, V.A., Babansky, A.D., Kovalenko, D.V., Kostitsin, Yu.A., Tolstykh, M.L., Kuscheva, Yu.A., 2017. The beginning of volcanic activity within Sredinny metamorphic Massif (Sredinny Range, Kamchatka). Dokl. Earth Sci. 475 (2), 858–862.

Plechov, P.Yu., 2008. Multiplicity of the Island Arc Magma Sources and Dynamic of Their Interaction. Dr. Sci. Thesis [in Russian]. MGU, Moscow.

Portnyagin, M., Duggen, S., Hauff, F., Mironov, N., Bindeman, I., Thirlwall, M., Hoernle, K., 2015. Geochemistry of the Late Holocene rocks from the Tolbachik volcanic field, Kamchatka: Quantitative modelling of subduction-related open magmatic systems. J. Volcanol. Geotherm. Res. 307, 133–155.

Portnyagin, M., Bindeman, I., Hoernle, K., Hauff, F., 2007. Geochemistry of primitive lavas of the Central Kamchatka Depression: Magma generation at the edge of the Pacific Plate, in: Eichelberger, J., Gordeev, E., Izbekov, P., Kasahara, M., Lees, J. (Eds.), Volcanism and Subduction: The Kamchatka Region. AGU, Washington, D.C., Vol. 172, 203–244.

Prueher, L.M., Rea, D.K., 2001. Tephrochronology of the Kamchatka-Kurile and Aleutian arcs: evidence for volcanic episodicity. J. Volcanol. Geotherm. Res. 106, 67–84.

Shapiro, M.N., Lander, A.V., 2003. Origin of the contemporary subduction zone in Kamchatka, in: Essays of Geophysical Research: to the

75th anniversary of the Schmidt Joint Institute of Physics of Earth [in Russian]. IPE RAS, Moscow, pp. 338–344.

Steiger, R.H., Jager, H., 1977. Subcommition on Geochronology: Convention on the use of decay constants in geo- and cosmochronology. Earth Planet. Sci. Lett. 36 (3), 359–362.

Sun, S.S., McDonough, W.F., 1989. Chemical and isotopic systematics of oceanic basalts; implications for mantle composition and processes, in: Saunders, A.D., Norry, M.J. (Eds.), Magmatism in the Ocean Basins. Geol. Soc. London Spec. Publ., pp. 313–345.

Tatsumi, Y., Kogiso, T., Nohda, S., 1995. Formation of a third volcanic chain in Kamchatka: generation of unusual subduction-related magmas. Contrib. Mineral. Petrol., 120, 117–128.

Turner, S.J., Langmuir, C.H., Dungan, M.A., Escrig, S., 2017. The importance of mantle wedge heterogeneity to subduction zone magmatism and the origin of EM1. Earth Planet. Sci. Lett. 472, 216–228.

Volynets, A., Churikova, T., Wörner, G., Gordeychik, B., Layer, P., 2010. Mafic Late Miocene–Quaternary volcanic rocks in the Kamchatka back arc region: implications for subduction geometry and slab history at the Pacific-Aleutian junction. Contrib. Mineral. Petrol. 159, 659–687.

Volynets, A.O., Pevzner, M.M., Tolstykh, M.L., Babansky, A.D., 2018. Volcanism of the southern part of the Sredinny Range of Kamchatka in the Neogene–Quaternary. Russian Geology and Geophysics (Geologiya i geofizika) 59 (12), 1577–1591 (1979–1996).

Volynets, O.N., 1993. Petrology and Geochemical Specialization of Volcanic Series of the Contemporary Island-Arc System. Dr. Sci. Thesis [in Russian]. MGU, Moscow.

Volynets, O.N., 1994. Geochemical types, petrology and genesis of late Cenozoic volcanic rocks from the Kurile-Kamchatka island-arc system. Int. Geol. Rev. 36, 373–405.

Editorial responsibility: A.E. Izokh